Nephelauxetic effect for the isoelectronic 3d3- ions (Cr3+, Mn4+, Fe5+) in SrTiO3

ARTICLE *in* JOURNAL OF PHYSICS AND CHEMISTRY OF SOLIDS · JULY 2006

Impact Factor: 1.85 · DOI: 10.1016/j.jpcs.2006.02.010

2 AUTHORS:

Mikhail G Brik
University of Tartu
397 PUBLICATIONS **2,387** CITATIONS
SEE PROFILE

Nicolae Avram
West University of Timisoara
140 PUBLICATIONS **836** CITATIONS
SEE PROFILE

Available online at www.sciencedirect.com
SCIENCE DIRECT
Journal of Physics and Chemistry of Solids 67 (2006) 1599–1604
JOURNAL OF PHYSICS AND CHEMISTRY OF SOLIDS
www.elsevier.com/locate/jpcs

Nephelauxetic effect for the isoelectronic $3d^3$-ions (Cr^{3+}, Mn^{4+}, Fe^{5+}) in $SrTiO_3$

M.G. Brik[a], N.M. Avram[b,*]

[a]Department of Chemistry, School of Science and Technology, Kwansei Gakuin University, 2–1 Gakuen, Sanda, Hyogo 669–1337, Japan
[b]Department of Physics, West University of Timisoara, Bd. V. Parvan No. 4, 300223, Timisoara, Romania

Received 14 December 2005; received in revised form 24 January 2006; accepted 14 February 2006

Abstract

The exchange charge model of crystal field theory has been used to analyze systematically the ground state absorption spectra of isoelectronic Cr^{3+}, Mn^{4+}, and Fe^{5+} ions in an octahedral coordination in the $SrTiO_3$ crystal. The parameters of the crystal field acting on the valence electrons of impurity ions are calculated from the available crystal structure data. A special attention is paid to the analysis of dependencies of the crystal field invariants and covalence effects on the impurity ion. It is shown numerically that the covalence effects between the above impurity ions and ligands increase with an increase of the 3d-ion oxidation state.

Keywords: D. Crystal fields; D. Optical properties

1. Introduction

Recently, several papers devoted to the optical properties of the $SrTiO_3$ (STO) crystal doped with transition metal ions have been published [1–3] (and references therein). Ref. [4] contains systematic analysis of the EPR g-factors of the isoelectronic $3d^3$ series (Cr^{3+}, Mn^{4+}, Fe^{5+}) in STO; in a consistent approach, trends in the EPR parameters related to the change of the central ion, have been discussed.

This paper is a consecutive continuation and development of our recent work [5], in which optical properties of the Ni^{2+} ion in isostructural $NiCl_2$, $NiBr_2$ and NiI_2 hosts were considered as a function of the ligands' atomic number. Specific choice of the considered systems in [5] (the central ion in the $[NiX_6]^{4-}$ cluster (X = Cl^-, Br^-, I^-) is the same; the ligands' charges are the same and the symmetry of all hosts is also the same) ensured eliminating all other factors excepting the nature of ligands. It was shown that the crystal field strength Dq [6], crystal field invariant [7,8] (and, therefore, splittings of the Ni^{2+} terms) decrease as the ligands' atomic number increases. In addition, the covalence effects and overlap integrals between the Ni^{2+} ion and ligands increase when increasing the ligands' atomic number and moving from $NiCl_2$ to NiI_2 through $NiBr_2$.

In the present paper consistent crystal field study (within the exchange charge model (ECM) [9] frameworks) is performed for the above isoelectronic $3d^3$ ions in STO. Considering only one host and changing the central ions gives an opportunity to see how the optical properties and crystal field parameters depend on the nature of the impurity ion: its charge and atomic number. We present here the calculations of the crystal field parameters (CFP), energy levels of the above mentioned ions in the STO crystal, and analyze how the energy levels and covalence effects change with changing an impurity ion.

We do not take into account the vibronic interactions and Jahn–Teller effect (we may emphasize that the data on the fine structure of the $^4T_{2g}$ state are scarse for these crystals, and for STO:Fe^{5+} no optical spectra at all were reported in the literature) and we focus our attention on crystal field studies only to see how changing of impurity ions influence the optical properties of the crystal.

*Corresponding author.
E-mail address: avram@physics.uvt.ro (N.M. Avram).

0022-3697/$ - see front matter © 2006 Elsevier Ltd. All rights reserved.
doi:10.1016/j.jpcs.2006.02.010

2. Crystal structure of STO and basic spectroscopic parameters of STO doped with Cr^{3+}, Mn^{4+}, Fe^{5+}

STO crystal has a perovskite type structure, space group Pm3m, lattice constant $a = 3.90528$ Å [10]. After doping, Cr^{3+} (Mn^{4+}, Fe^{5+}) substitute for Ti^{4+} ion at the center of the oxygen octahedron (Fig. 1).

Concerning the optical properties of ions from the above series in STO, the literature data differ significantly (Table 1). For example, the Racah parameter B and crystal field strength Dq in for STO:Cr^{3+} in [11] are given (in cm^{-1}) as 750 and 1879, respectively, whereas the authors of [12] give the values of 560 and 1530 (differing by 25% and 19%, respectively). No d–d transitions have been reported in the optical spectra of STO:Fe^{5+} [4], and the authors of Ref. [4] just estimated their values using the extrapolating method from the values for STO:Cr^{3+} and STO:Mn^{4+}. For the sake of consistency, we adopted in our calculations the values of Dq, B and C suggested in [4]. They were shown to give a very good agreement between the calculated and measured EPR parameters. We will mainly concentrate on the trends existing between STO crystals doped with considered ions, and *absolute* agreement with experimental spectra (especially taking into account the broad absorption bands of 3d ions in crystals and lack of well defined spectroscopic parameters, as illustrated by Table 1) is not the aim of the present study.

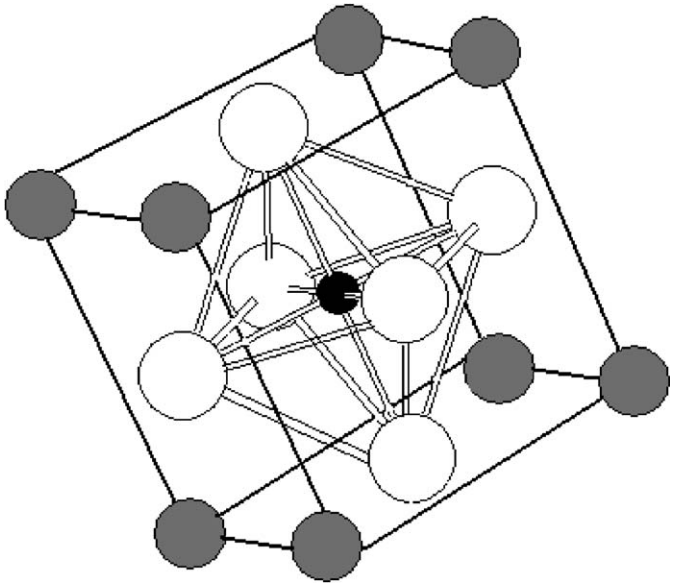

Fig. 1. Crystal structure of $SrTiO_3$. Oxygen ions are shown by white circles, strontium—by grey, and titanium—by small black one. Octahedron formed by six oxygen ions around Ti^{4+} ion (which is substituted for by Cr^{3+}, Mn^{4+}, and Fe^{5+} ions, is also shown).

Table 1
Spectroscopic parameters (in cm^{-1}) of STO:Cr^{3+}, STO:Mn^{4+}, and STO:Fe^{5+}

	STO:Cr^{3+}			STO:Mn^{4+}		STO:Fe^{5+}
B	750	560	662	719	735	800
C	–	–	2587	2839	2816	3050
Dq	1879	1530	1618	1818	1821	2020
Ref.	[11]	[12]	[4]	[1]	[4]	[4]

3. Crystal field calculations for STO:Cr^{3+} (Mn^{4+}, Fe^{5+}): description of the method and discussion of the results

Energy levels of impurity ions in this work are represented by the eigenvalues of the following crystal field Hamiltonian [9]:

$$H = \sum_{p=2,4} \sum_{k=-p}^{p} B_p^k O_p^k, \tag{1}$$

where O_p^k are the linear combinations of irreducible tensor operators acting on angular parts of the 3d-ion wave functions, and B_p^k are CFP containing all information about geometrical arrangement of the ligands around the central ion. Following Ref. [9], these parameters can be written as a sum of two terms:

$$B_p^k = B_{p,q}^k + B_{p,S}^k. \tag{2}$$

The former contribution originates from the electrostatic interaction between valence electrons of an impurity ion and ions of crystal lattice (treated as the point charges, without taking into account their electron structure). The latter is proportional to the overlap of the wave functions of an impurity ion and ligands; it includes effects of the covalent bond formation and exchange interaction. Inclusion of these effects significantly improves an agreement between the calculated and experimentally observed energy levels. Expressions for calculating both contributions to the CFP in the case of 3d-ion are as follows [9]:

$$B_{p,q}^k = -K_p^k e^2 \langle r^p \rangle \sum_i q_i \frac{V_p^k(\theta(i), \varphi(i))}{R(i)^{p+1}}, \tag{3}$$

$$B_{p,S}^k = K_p^k e^2 \frac{2(2p+1)}{5} \times \sum_i \left(G_s S_s(i)^2 + G_\sigma S_\sigma(i)^2 + \gamma_p G_\pi S_\pi(i)^2 \right) \times \frac{V_p^k(\theta(i), \varphi(i))}{R(i)}. \tag{4}$$

The sums are carried out over lattice ions denoted by i with charges q_i (expressed in units of the electron charge e); $R(i)$, $\theta(i)$, $\varphi(i)$ are the spherical coordinates of the ith ion of crystal lattice in the system of reference centered at the impurity ion. The averaged values $\langle r^p \rangle$ of pth power of the impurity ion electron radial coordinate can be found in Ref. [13], or easily calculated using the wave functions of the 3d-ions given in [14]. The values of the numerical factors K_p^k, γ_p and expressions for the polynomials V_p^k are all given in [9]. S_s, S_σ, S_π stand for the overlap integrals between d-functions of the central ion and p- and

Table 2
Overlap integrals between Cr^{3+} (Mn^{4+}, Fe^{5+}) and O^{2-} ions in STO ($3.0<r<4.0$ atomic units) and averaged values of $\langle r^2\rangle$ and $\langle r^4\rangle$ (in a.u.) calculated with wave functions from [14]

	STO:Cr^{3+}	STO:Mn^{4+}	STO:Fe^{5+}
$S_s=\langle d0\|s0\rangle$	$-0.90111\exp(-0.59683r)$	$-0.92125\exp(-0.69807r)$	$-1.00200\exp(-0.81119r)$
$S_\sigma=\langle d0\|p0\rangle$	$-0.83835\exp(-0.64118r)$	$0.85114\exp(-0.74151r)$	$0.90092\exp(-0.84777r)$
$S_\pi=\langle d1\|s1\rangle$	$-1.54570\exp(-0.91718r)$	$1.46440\exp(-1.10230r)$	$1.27430\exp(-1.09140r)$
$\langle r^2\rangle$	1.43402	1.09876	0.88073
$\langle r^4\rangle$	4.262822	2.401200	1.50154

s-functions of the ligands (they correspond to the following integrals (in $\langle lm|l'm'\rangle$ notation): $S_s=\langle d0|s0\rangle$, $S_\sigma=\langle d0|p0\rangle$, $S_\pi=\langle d1|p1\rangle$). G_s, G_σ, G_π are dimensionless adjustable parameters of the model determined from the positions of the first three absorption bands. For practical purposes, it is sufficient to assume them to be equal to each other: $G_s=G_\sigma=G_\pi=G$ (in this case only the first absorption band is required to determine the value of G); this simplified model is used in the present paper. The strong advantage of the ECM is that if the G parameter is determined to fit the first absorption band, the other energy levels, located higher in energy, will also fit experimental spectra fairly well.

The ECM has been successfully applied for the calculations of the energy levels of both rare earth [9,15–18] and transition metal ions in different hosts as well [19–28] and analysis of the electron-phonon coupling and non-radiative transitions [29–31].

When calculating CFP, a special attention should be paid to the convergence of the lattice sums in Eq. (3). As a first approximation, it is possible to consider the nearest ligands only, but since the second rank point charges parameters $B^k_{2,q}$ decrease not so fast as the fourth rank parameters $B^k_{4,q}$ (as $1/R^3$ and $1/R^5$, respectively), the contribution of the ligands from the second and further coordination spheres can be quite significant. To increase accuracy in calculating the point charge contribution to the CFP, large cluster consisting of 1 Cr^{3+} (or Mn^{4+}, or Fe^{5+}) ion, 123 Sr^{2+} ions, 135 Ti^{4+} ions and 336 O^{2-} ions were considered. This cluster enables to take into account the contribution of ions located at the distances at least up to 15 Å from the central ion. For the exchange charge parameters (Eq. (4)) only the nearest ligands were taken into account, since the overlap between an impurity ion and ligands from other than the first coordination sphere can be safely neglected. The overlap integrals between the Cr^{3+} (Mn^{4+}, Fe^{5+}) and O^{2-} ions needed for calculating the exchange charge contribution $B^k_{p,S}$ to the CFP were computed numerically using the radial wave functions of the above mentioned ions given in [14,32], respectively. The dependences of the overlap integrals on the interionic distance r (r is measured in atomic units) were approximated by the exponential functions given in Table 2. For the exchange charge parameters (Eq. (4)) only the nearest ligands were taken into account, since the overlap between an impurity ion and ligands (decreasing exponentially with increasing distance) from other than the first coordination sphere can be safely neglected.

Table 3
Crystal field parameters (in cm^{-1}) for Cr^{3+}, Mn^{4+}, and Fe^{5+} in the STO crystal

Large cluster (1 Cr^{3+} (or Mn^{4+}, or Fe^{5+}) ion, 123 Sr^{2+} ions, 135 Ti^{4+} ions and 336 O^{2-} ions)			
Crystal field parameter	Cr^{3+}	Mn^{4+}	Fe^{5+}
B^{-2}_2	−0.1	0	0
B^{-1}_2	−0.1	−0.1	−0.1
B^0_2	0	0	0
B^1_2	−0.1	−0.1	−0.1
B^2_2	0	0	0
B^{-4}_4	0	0	0
B^{-3}_4	2.8	1.6	1.0
B^{-2}_4	0.8	0.5	0.3
B^{-1}_4	−0.4	−0.2	−0.1
B^0_4	4247.4	4780.1	5302.8
B^1_4	−0.4	−0.2	−0.1
B^2_4	0	0	0
B^3_4	−2.8	−1.6	−1.0
B^4_4	21237.1	23900.4	26513.8
Crystal field parameter N_v, Eq. (5)	25591	28801	31950
Small cluster (1 Cr^{3+} (or Mn^{4+}, or Fe^{5+}) ion and 6 O^{2-} ions)			
B^0_4	4235	4773	5298
B^4_4	21173	23864	26491
Crystal field parameter N_v, Eq. (5)	25514	28757	31923

The CFP values obtained after using Eqs. (1)–(4), exponential functions from Table 2 for the overlap integrals and crystal structure data from [10] (which enable to get the Cartesian coordinates of the ligands in the system of reference defined with respect to the crystallographic axes) are shown in Table 3. The last row of Table 3 shows the values of the scalar crystal field parameter N_v defined as [7,8]

$$N_v=\left[\sum_{p,k}\left(B^k_p\right)^2\frac{4\pi}{2p+1}\right]^{1/2}. \quad (5)$$

Table 3 also contains the results of the CFP calculations for small clusters, when only nearest six ions of oxygen are considered. The values of the CFP are different for small

Table 4
Crystal field splittings of the lowest spin-quartet terms ^4F and ^4P (in cm^{-1}) for Cr^{3+}, Mn^{4+}, and Fe^{5+} in $SrTiO_3$

O_h irred. repres.	Cr^{3+}	Mn^{4+}	Fe^{5+}
$^4A_{2g}$ (^4F)	0	0	0
$^4T_{2g}$ (^4F)	16181	18210	20201
$^4T_{1g}$ (^4F)	22764	25544	28221
$^4T_{1g}$ (^4P)	35710	40112	44382

and large clusters; this difference is much more significant when low-symmetry centers are considered, when the contribution of the second rank CFP is non-zero [21,28]. It is also worthwhile to point out that inclusion of the exchange charge contribution (Eq. (4)) into the calculations of the CFP is very important for getting a reasonambe agreement between the calculated and observed energy levels. As shown in refs. [21–28], the point charge contribution (Eq. (3)) is only from 20 to 50% of the total value, and the remaining contribution is due to the exchange effects (Eq. (4)).

The crystal field Hamiltonian (1) was diagonalized in the space spanned by 10 wave functions of the lowest spin-quartet ^4F, ^4P terms of the $3d^3$ electron configuration. The adjustable parameter G was defined by fitting the calculated position of the first spin-allowed $^4A_{2g}$–$^4T_{2g}$ absorption band to the value of $10Dq$ and turned out to be 2.608, 6.154, and 15.370 for STO:Cr^{3+}, STO:Mn^{4+}, and STO:Fe^{5+}, respectively. Finally, the obtained energy levels are listed in Table 4.

Regarding the CFP values, as follows from Table 3, the main contribution to the Hamiltonian (1) is produced by B_4^0 and B_4^4 parameters, with all others having very small values. This suggests the role of the low-symmetry component of crystal field in STO to be very weak. As seen from Table 3, CFP increase monotonically as a function of the atomic number of an impurity ion in STO, and so does the crystal field parameter N_v.

Splitting of the spin-quartet terms also follow the same trend (Table 4), and this is another justification of increasing crystal field strength when going from Cr^{3+} to Mn^{4+}, and, finally, Fe^{5+} in STO.

It is interesting to analyze how the bilinear form constructed from the overlap integrals (Eq. (4)) depends on the central ion atomic number. Figs. 2 and 3 show the bilinear forms S_2 and S_4, respectively, as the functions of the "3d ion – ligand" distance for all three considered ions in the STO crystal. As shown by Figs. 2 and 3, the bilinear forms S_2 and S_4 for Fe^{5+} are dominating, those for Cr^{3+} always take the smallest values, and those for Mn^{4+} are always between these two. This is a clear indication that the covalence of the chemical bonds between central ion and ligands in the STO increases with increasing the central ion atomic number (or, what is the same in this case, its electrical charge). Even if the ionic radii of 3d ions decrease with increasing atomic number [33] (see also Table 2, in

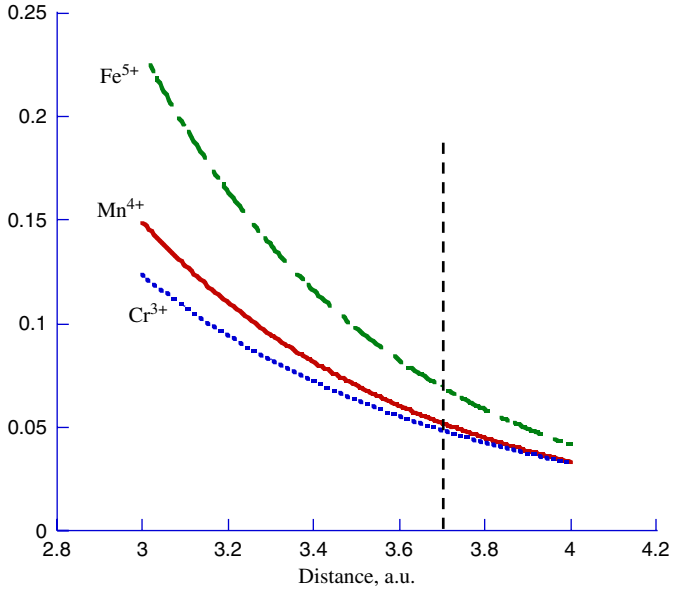

Fig. 2. Dependence of $S_2 = G(S_s(i)^2 + S_\sigma(i)^2 + \gamma_2 S_\pi(i)^2)$, $\gamma_2 = 1$ for Cr^3, Mn^{4+}, Fe^{5+} on distance. Position of STO crystal with the "central ion – ligand" separation of 3.69 a.u. is shown by vertical dashed line.

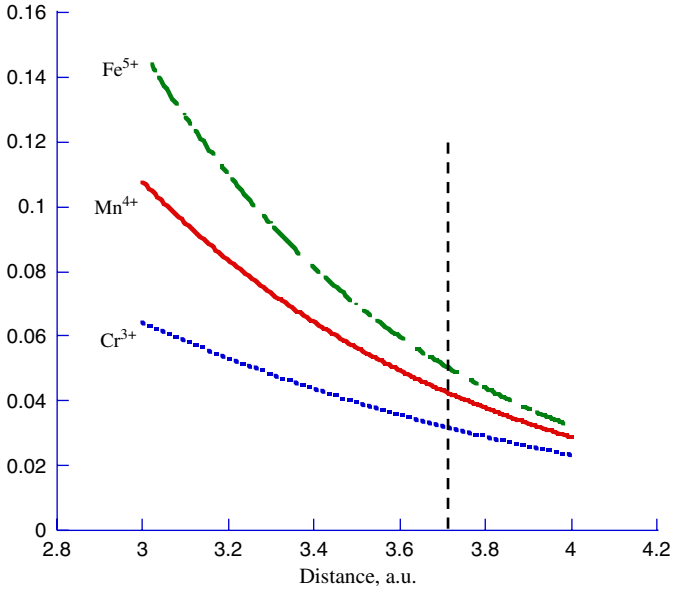

Fig. 3. Dependence of $S_4 = G(S_s(i)^2 + S_\sigma(i)^2 + \gamma_4 S_\pi(i)^2)$, $\gamma_4 = -4/3$ for Cr^{3+}, Mn^{4+}, Fe^{5+} on distance. Position of STO crystal with the "central ion – ligand" separation of 3.69 a.u. is shown by vertical dashed line.

which the averaged powers $\langle r^2 \rangle$ and $\langle r^4 \rangle$ of the 3d electron radial coordinate monotonically decrease with increasing atomic number), increasing electric charge of the central ion causes re-distributing of the electron density around central ion with increasing contribution of the ligands wave functions and making the chemical bond between the central ion and ligands "more covalent".

The role played by covalence effects in the considered systems can be analyzed from another point of view, using

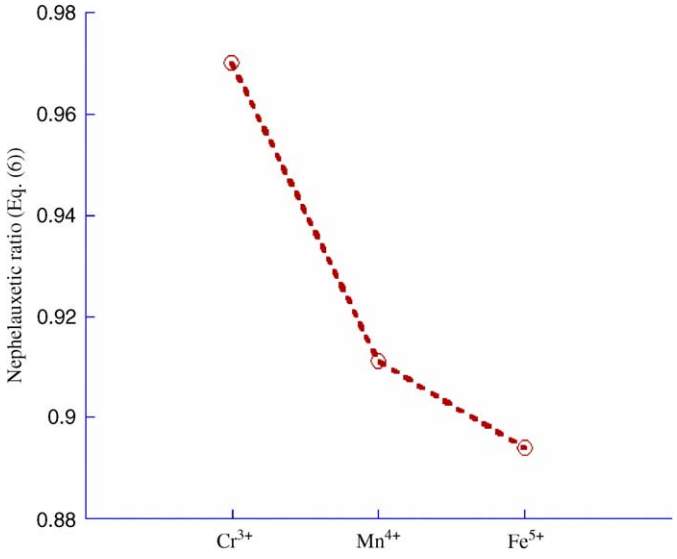

Fig. 4. Nephelauxetic ratio β (Eq. (6)) for Cr^{3+}, Mn^{4+}, and Fe^{5+} in the STO crystal.

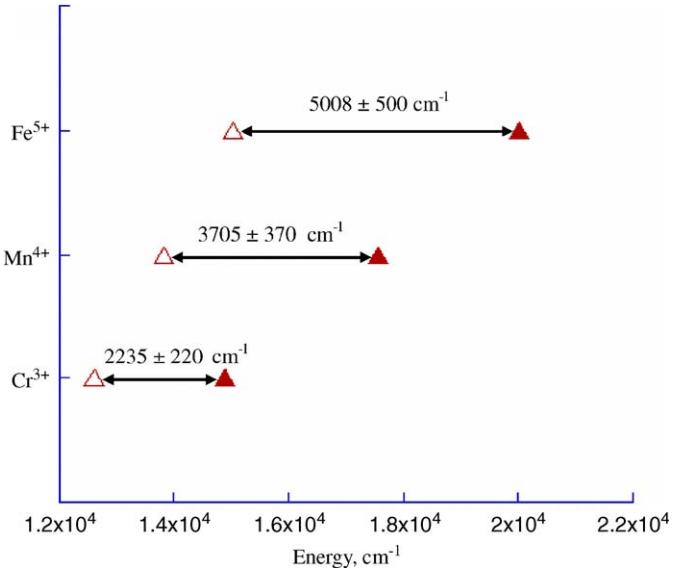

Fig. 5. Energies of the first spin-forbidden transition $^2E(^2G)$–$^4A_{2g}(^4F)$ of Cr^{3+}, Mn^{4+}, Fe^{5+} ions in the STO crystal (open triangles) with respect to the energies of the first spin-forbidden transition ^2G–^4F of free Cr^{3+}, Mn^{4+}, Fe^{5+} ions (filled triangles). The experimental errors are not known but we assume the deviation from the calculated values to be about 10% (above the arraws), what cover well any experimental errors.

the following non-dimensional quantity;

$$\beta = \sqrt{\left(\frac{B_1}{B_0}\right)^2 + \left(\frac{C_1}{C_0}\right)^2}, \quad (6)$$

where subscripts "1" and "0" are related to the values of the Racah parameters in a crystal and in a free state, respectively. This quantity can serve as a qualitative measure of the nephelauxetic effect (significant decrease of the Racah parameters for 3d ions in a crystal with respect to those in a free state). For free Cr^{3+} ion these parameters are $B = 995\,cm^{-1}$, $C = 3637\,cm^{-1}$ [34], for free Mn^{4+} they are $B = 1160\,cm^{-1}$, $C = 4303\,cm^{-1}$ [34], an for free Fe^{5+} they can be estimated from data presented in [35] as $B = 1210\,cm^{-1}$, $C = 5066\,cm^{-1}$. Dependence of β on the type of impurity ion is shown in Fig. 4. It decreases monotonically with increasing central ion atomic number, thus showing covalence effects to play more and more significant role when going from Cr^{3+} to Fe^{5+} in the STO crystal. As follows from the Dq/B ratio, all considered 3d ions experience strong crystal field in the STO crystal (when the first excited state is the spin-doublet $^2E(^2G)$). Therefore, in the luminescence spectra of the STO crystals doped with Cr^{3+}, Mn^{4+}, Fe^{5+} there should be sharp R-lines [1,11,12]. Fig. 5 shows the comparison of the $^2E(^2G)$–$^4A_{2g}(^4F)$ energy difference of Cr^{3+}, Mn^{4+}, Fe^{5+} ions in the STO crystal (calculated using the complete d^3 configuration energy matrix in the cubic field [36] with respect to the energies of the first spin-forbidden transition ^2G–^4F of free Cr^{3+}, Mn^{4+}, Fe^{5+} ions. There is monotonic increase of both energies with increasing of the 3d ion atomic number, and it is obviously related to the increase of the corresponding Racah parameters. On the other hand, the energies of the first spin-forbidden transitions decrease significantly, when an impurity ion is placed into the STO crystal. The magnitude of such a decrease (shown in Fig. 5 by the numbers above arrows) grows up with increasing 3d ion atomic number, again showing more significant decrease of the Racah parameters (and, correspondingly, nephelauxetic effect) for 3d ions with greater atomic number and oxidation state.

All these estimations quantitatively confirm the trend in the spectra of the isoelectronic series of 3d-ions in the same crystal, namely: increase of the Dq, B, and C parameters due to increase of the covalence and electric charge of 3d-ions [37].

4. Conclusion

Consistent crystal field analysis of the energy level splittings and covalence effects for the STO crystal doped with Cr^{3+}, Mn^{4+}, Fe^{5+} ions was performed within the ECM framework. Specific choice of the activator ions (all of them have the same $3d^3$ electron configuration and are placed into the same host matrix) ensured eliminating all effects other than the atomic number (or, in other words, the electric charge of the impurity ion). Crystal structure data were used to calculate the CFP values, which were used then to calculate the splittings of the lowest terms of all considered ions. Reasonable agreement between the calculated and measured crystal field splittings confirms validity of the results obtained in the paper. It was shown that both crystal field strength and covalence in all considered systems increase with increasing 3d-ion atomic number, such an increase is accompanied by a decrease in the Racah parameters of these ions with respect to those for a free state (or decrease of the nephelauxetic parameter β defined by Eq. (6)).

The main results of the present paper are closely connected with main conclusions obtained in [5]. In that paper, dependencies of the spectral properties of Ni^{2+} ions in three isostructural hosts ($NiCl_2$, $NiBr_2$, NiI_2) were studied as the functions of the ligand atomic number. The covalency and nephelauxetic effects were shown to increase with increasing atomic number. So, paper [5] and the present paper are closely related to each other.

It should be mentioned here that electron–vibronic interaction (in particular, the Jahn–Teller effect), which plays important role in formation of optical properties of 3d ions in crystals, has been left out of consideration in this paper. There are several reasons for that: first of all, experimental results available in the literature, demonstrate a lack of data regarding fine structure of the energy levels (spin–orbit splitting, which can be used for estimation of the Jahn–Teller stabilization energy) and frequencies of the normal vibrations in the STO crystal. Second, the main aim of the paper was to perform systematic analysis of the effects caused by overlapping of the impurity ion and ligands wave functions and formation of the covalent bonds between these ions. Third, since only impurity ions are varied (but their electronic configuration is the same), host dynamics influence contributes to the same extent in each case and does not affect significantly the main conclusions of the paper.

Another observation is related to the possible effects of interaction between an impurity center formed by 3d ion and the whole crystal matrix. An impurity center can be treated as a nanocluster which is incorporated into the host crystal (like it was done for the TiO6 octahedra in [38]). It was shown in [38] that these ''cluster-related incorporating effects'' are very important for the formation of non-linaer optical properties and intensities of the optical transitions. These effects are not considered here, but may add significant information to the properties of the STO crystal doped with transition metal ions.

Acknowledgment

M.G. Brik thanks the members of Computational Materials Science Unit in Kyoto University for helpful discussion.

References

[1] Z. Bryknar, V. Trepakov, Z. Potucek, L. Jastrabic, J. Lumin. 87–89 (2000) 605.
[2] V.A. Trepakov, I.B. Kudyk, S.E. Kapphan, M.E. Savinov, A. Pashkin, L. Jasrtrabik, A. Tkach, P.M. Vilarinho, A.L. Kholkin, J. Lumin. 102–103 (2003) 536.
[3] A. Yamanaka, M. Kataoka, Y. Inaba, K. Inoe, B. Hehlen, E. Courtens, Europhys. Lett. 50 (2000) 688.
[4] W.-C. Zheng, X.-X. Wu, J. Phys. Chem. Solids 66 (2005) 1701.
[5] M.G. Brik, N.M. Avram, C.N. Avram, Physica B 371 (2006).
[6] S. Sugano, Y. Tanabe, H. Kamimura, Multiplets of Transition-Metal Ions in Crystals, Academic Press, New York, 1970.
[7] F. Auzel, O. Malta, J. Phys. 44 (1983) 201.
[8] F. Auzel, Opt. Mater. 19 (2002) 89.
[9] B.Z. Malkin, in: A.A. Kaplyanskii, B.M. Macfarlane (Eds.), Spectroscopy of Solids Containing Rare-earth Ions, North-Holland, Amsterdam, 1987, pp. 33–50.
[10] R.H. Mitchell, A.R. Chakhmouradian, P.M. Woodward, Phys. Chem. Minerals (Germany) 27 (2000) 583.
[11] L. Rimai, T. Deutsch, B.D. Silverman, Phys. Rev. 133 (1964) A1123.
[12] S.E. Stokowski, A.L. Schawlow, Phys. Rev. 178 (1969) 457.
[13] A.G. Abragam, B. Bleaney, Electron Paramagnetic Resonance of Transition Ions, Oxford, Clarendon, 1970.
[14] E. Clementi, C. Roetti, Atomic Data and Nuclear Data Tables 14 (1974) 177.
[15] G.A. Bogomolova, L.A. Bumagina, A.A. Kaminskii, B.Z. Malkin, Fizika Tverdogo Tela (Sov. Phys. Sol. Stat.) 19 (1977) 1439.
[16] M.N. Popova, S.A. Klimin, E.P. Chukalina, R.Z. Levitin, B.V. Mill, B.Z. Malkin, E. Antic-Fidancev, J. Alloys Compounds 380 (2004) 84.
[17] M.N. Popova, E.P. Chukalina, B.Z. Malkin, A.I. Iskhakova, E. Antic-Fidancev, P. Porcher, J.P. Chaminade, Phys. Rev. B 63 (2001) 075103.
[18] M.N. Popova, S.A. Klimin, E.P. Chukalina, E.A. Romanov, B.Z. Malkin, E. Antic-Fidancev, B.V. Mill, G. Dhalenne, Phys. Rev. B 71 (2005) 024414.
[19] M.G. Brik, C.N. Avram, N.M. Avram, in: Martin E. Fermann, Larry R. Marshall, (Eds.), OSA Trends in Optics and Photonics, vol. 68, Advanced Solid-State Lasers, Optical Society of America, Washington, DC 2002, pp. 275–279.
[20] C. Jousseaume, D. Vivien, A. Kahn-Harari, B.Z. Malkin, Opt. Mater. 24 (2003) 143.
[21] M.G. Brik, N.M. Avram, Z. Naturf. 59a (2004) 799.
[22] M.G. Brik, C.N. Avram, I. Tanaka, Phys. Stat. Sol. B 241 (2004) 2501.
[23] M.G. Brik, N.M. Avram, C.N. Avram, Sol. Stat. Commun. 132 (2004) 831.
[24] M.G. Brik, N.M. Avram, C.N. Avram, I. Tanaka, Eur. Phys. J. Appl. Phys. 29 (2005) 239.
[25] M.G. Brik, Z. Naturf. 60a (2005) 606.
[26] A. El-Korashy, M.G. Brik, Sol. Stat. Commun. 135 (2005) 298.
[27] M.G. Brik, N.M. Avram, C.N. Avram, Centr. Eur. J. Phys. 3 (2005) 508.
[28] M.G. Brik, N.M. Avram, C.N. Avram, Spectrochim. Acta A 63 (2006) 759.
[29] S.I. Klokishner, B.S. Tsukerblat, O.S. Reu, A.V. Palii, S.M. Ostrovsky, Opt. Mater. 27 (2005) 1445.
[30] M.N. Popova, E.P. Chukalina, B.Z. Malkin, S.K. Saikin, Phys. Rev. B 61 (2000) 7421.
[31] S.I. Klokishner, B.S. Tsukerblat, O.S. Reu, A.V. Palii, S.M. Ostrovsky, Chem. Phys. 316 (2005) 83.
[32] M.V. Eremin, in: Spectroscopy of Crystals (in Russian), Moscow, 1989, pp. 30–44.
[33] R.D. Shannon, Acta Cryst. A 32 (1976) 751.
[34] P.H.M. Uylings, A.J.J. Raassen, J.F. Wyart, J. Phys. B 17 (1984) 4103.
[35] http://physics.nist.gov—National Institute of Standards and Technology, Physics Laboratory website, Atomic Spectroscopy Data.
[36] W.A. Runciman, K.A. Schroeder, Proc. Roy. Soc. (London) A 265 (1962) 489.
[37] A.B.P. Lever, Inorganic Electronic Spectroscopy, Elsevier Press, Amsterdam, 1984.
[38] I.V. Kityk, A. Majchrowski, B. Sahraoui, Opt. Lasers Eng. 43 (2005) 75.